Vol. 38: 43–59, 2008
doi: 10.3354/cr00758

CLIMATE RESEARCH
Clim Res

Printed December 2008
Published online November 18, 2008

OPEN ACCESS

Downscaling experiment for the Venice lagoon. II. Effects of changes in precipitation on biogeochemical properties

G. Cossarini[1], S. Libralato[1], S. Salon[1], X. Gao[2,3], F. Giorgi[2], C. Solidoro[1,*]

[1]**Department of Oceanography, Istituto Nazionale di Oceanografia e di Geofisica Sperimentale – OGS, Borgo Grotta Gigante-Briščiki 42/c, 34010 Sgonico-Zgonik (Trieste), Italy**
[2]**Earth System Physics Group, The Abdus Salam International Centre for Theoretical Physics – ICTP, Strada Costiera 11, 34014 Trieste, Italy**
[3]**National Climate Center of China, Beijing 100081, China**

ABSTRACT: A downscaling approach is used to assess potential effects of variations in nutrient loads induced by possible future climate changes on biogeochemical properties of the Venice lagoon. The analysis is based on a hierarchy of dynamic and statistical models linking climatic change to effects on biogeochemical processes. The outputs of regional climate model simulations for present day and future (A2 and B2 IPCC emission scenarios) conditions are used to force 2 statistical models that provide forcing and boundary conditions for a 3D coupled transport-biogeochemical model of the lagoon. Results in terms of spatio-temporal dynamics of biogeochemical properties provide evidence of significant impacts of climate change. Under both the A2 and B2 scenarios, we observe an amplification of the seasonal precipitation patterns, with drier summers and wetter winters, which affect the timing of nutrient inputs to the lagoon. Nutrient loads are generally higher in the wintertime and lower in the summertime than in present-day conditions. In winter, nutrients are not used by phytoplankton whose productivity is low, and are mainly exported from the system. Conversely, reduced nutrient inputs to the lagoon in summer cause a reduction in planktonic productivity of the ecosystem. Between the 2 emission scenarios, the A2, which has higher levels of atmospheric greenhouse gas concentrations, shows more intense impact. Analysis of the effects of additional scenarios indicates that policy-driven changes in nutrient loads can overbalance changes due to climate driven modification of precipitation patterns.

KEY WORDS: Downscaling · Scenario analysis · Biogeochemical impacts · Venice lagoon

1. INTRODUCTION

The literature on potential impacts of anthropogenic climate change has markedly grown in the last decade (Howarth et al. 2000, Stenseth et al. 2002, Scavia et al. 2003, Harley et al. 2006). Among such impacts are modifications in river runoff induced by changes in precipitation patterns and their consequences on ocean biogeochemistry (Najjar et al. 2000, Lehman 2004, Struyf et al. 2004). Although modifications of freshwater discharge can influence nutrient dynamics through modification of water column stratification (Howarth et al. 2000, Justić et al. 2005), changes in the timing and volume of freshwater and nutrient delivery are also critical in coastal shallow areas such as wetlands (Scavia et al. 2003). While the total amount of nutrients generated in the drainage basin largely depends on land use (farming, urban wastes and other anthropogenic discharges; Bouwman et al. 2005), precipitation regimes can significantly affect the fraction of nutrients transported to the water body and its seasonal pattern (Najjar 1999). These factors in turn can

*Corresponding author. Email: csolidoro@inogs.it

deeply affect nutrient dynamics (Boesch et al. 2000, Neff et al. 2000).

Consequently, water quality and trophic state of coastal ecosystems might be significantly modified by climatic changes through variations in precipitation patterns. However, the inherent difficulties in predicting the direction and magnitude of changes in nutrient loads and their effects on coastal areas make this topic one of the least studied effects of climate change (Howarth et al. 2000, Scavia et al. 2003).

This study aims to assess potential impacts of changes in seasonal precipitation patterns on the biogeochemical properties of coastal areas using the Venice lagoon, Italy, as a case study. This lagoon is a highly productive ecosystem, where spatial distributions and time variability of biogeochemical properties are mostly influenced by river runoff and lagoon–sea exchanges (Solidoro et al. 2005a). To carry out our assessment, we implemented a downscaling framework involving 4 components: (1) a regional climate model (RCM) (Gao et al. 2006) that provides precipitation input for 2 statistical models, (2) and (3), which in turn provide boundary conditions for (4) a coupled transport-biogeochemical model of the lagoon (Solidoro et al. 2005b). Validation of the RCM precipitation patterns for the study area is reported in the companion paper by Salon et al. (2008, this issue).

This paper is organized as follows: Section 2.1 describes the Venice lagoon and introduces all data used for calibrating and validating the models; Sections 2.3 to 2.6 illustrate the models; Section 2.7 presents climate scenarios implemented in this study; Section 3.1 shows the results of the present climate scenario using the hierarchy of models; Sections 3.2 to 3.5 compare 4 future scenarios and present-day conditions and some conclusions are drawn in Section 4.

2. DATA AND METHODS

2.1. Study site and experimental data

The Venice lagoon is the largest lagoon in the Mediterranean Sea. It is located in the northern Adriatic Sea and has an area of 390 km^2. Its average depth is ~1 m, but its morphology is characterized by large shallow areas and a network of deeper navigable channels (Fig. 1). Three narrow inlets connect the lagoon to the Adriatic Sea. The lagoon receives $>5.5 \times 10^6$ kg of nitrogen and 0.4×10^6 kg of phosphorus per year from the drainage basin (10 rivers, a sewage treatment plant), which is highly urbanized and intensively farmed. In addition, port and industrial activities located on the lagoon shores have a negative impact on the water and sediment quality of this ecosystem (Bettiol et al. 2005, Suman et al. 2005). Despite this, the lagoon still hosts highly valuable typical habitats as well as several economic activities which depend on ecosystem health, such as fisheries, aquaculture, recreational activities and tourism.

Data on freshwater discharges and nutrient input from the 10 rivers, the sewage treatment plant, the industrial area of Porto Marghera and the city of Venice, are provided by local authorities and refer to comprehensive information gathered in the period 2001–2003 (CVN 2005). Nutrient measurements in the lagoon waters are available from a monitoring pro-

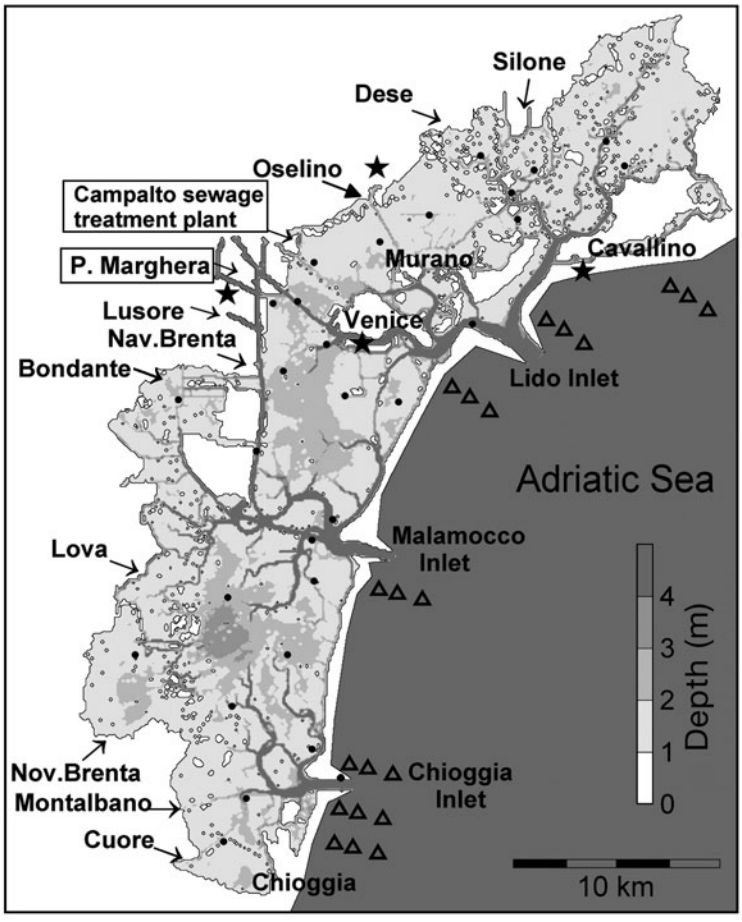

Fig. 1. Bathymetry of the Venice lagoon. Arrows and related names indicate riverine inputs. Urban areas discharging into the lagoon and the 3 inlets are also shown. Sewage treatment plant and industrial area are boxed. (●) Sampling locations for chemical and biological measurements (MELa; Solidoro et al. 2005a), (△) sampling locations of coastal water monitoring (Aubry et al. 2004), and (★) location of the 4 meteorological stations closest to the lagoon out of 20 stations in the lagoon drainage basin

gram called MELa (Solidoro et al. 2005a). During the MELa program, nutrients (DIN or dissolved inorganic nitrogen, i.e. the sum of nitrate [NO_3^-] and ammonia [NH_4^+]); and phosphate [PO_4^{3-}]), chlorophyll and temperature were measured monthly in 30 sampling locations (dots in Fig. 1) for the years 2001–2005. Measurements of nutrients and chlorophyll along the coastline in front of the lagoon were taken monthly during the period 1991–2004 (Aubry et al. 2004), in 21 sampling stations (triangles in Fig. 1).

Meteorological data consist of time series of temperature, wind, pressure, cloud cover, irradiance and humidity registered at 20 automatic recording stations spread over the drainage basin of the Venice lagoon. Fig. 1 shows the location of 4 of the 20 stations. Meteorological data are used to validate the RCM and to build regressions in statistical models and are extensively presented in the companion paper by Salon et al. (2008).

2.2. Numerical experiment scheme

As mentioned, the hierarchy of models implemented in this study consists of 4 components represented schematically in Fig. 2: (1) a regional climate model (RCM) providing inputs for 2 statistical models, (2) and (3), which in turn provide boundary conditions for a coupled transport-biogeochemical model (TDM) of the Venice lagoon (4).

The RCM provides the daily evolution of rainfall data over the watershed to the 2 statistical models. These in turn provide the daily evolution of boundaries for the TDM, namely the nutrient loads from the watershed (2) and the concentration for the state variables at the boundary between the lagoon and the sea (3). Further, the daily evolution of solar radiation, humidity, air temperature, and cloud cover from the RCM are used directly to force the heat budget module of the TDM to compute the water temperature and also for photosynthesis parameterization.

We use meteorological data extracted from the output of 3 multidecadal RCM simulations (Gao et al. 2006), one for the present-day period of 1961–1990 (hereafter referred to as RF experiment), and 2 future scenario simulations for the period 2071–2100 under the A2 and B2 emission scenarios of IPCC (2000), in which the CO_2 concentration increases to ~850 and 600 ppm by 2100, respectively.

2.3. The trophic diffusive model (TDM)

Dynamics of biogeochemical properties of the lagoon are simulated by a 3D coupled physical and biogeochemical model governing the evolution of 13 state variables in space and time. Transport processes are described by a simplified version of the advection diffusion equation (Dejak et al. 1998). Since we are interested in time scales much longer than the tidal scale, residual currents are considered in the advection diffusion scheme. As a consequence, diffusion is modified to embed effects of tidal agitation and the eddy diffusion coefficient is replaced by anisotropic space-varying eddy diffusivity tensors (Dejak et al. 1998). The advantage of this procedure is the acceptability of the computational cost of the simulation even for multidecadal runs since residual currents in the Venice lagoon are negligible (additional details in Solidoro et al. 2005b).

The biogeochemical state variables include a pool of phytoplankton (Phy), zooplankton (Zoo), DIN, PO_4^{3-}, nutrient content in detritus and sediments, and dissolved oxygen. The microbial loop is considered implicitly in the parameterization of recycling processes. The model is kept as simple as possible, but it can simulate the essential features of the seasonal cycles of nitrogen, phosphorus and dissolved oxygen satisfactorily. Fig. 3 shows the TDM specifying the state variables, forcings, interactions and boundaries used.

The model is forced by meteorological parameters including irradiance, wind speed, humidity, cloud cover and air temperature, which determine the water-air heat budget computed by a specific module. Irradiance also influences nutrient cycles directly by driving photosynthetic activity of the phytoplankton community, which in turn is forced by nutrient loads from rivers and urban point sources (black arrows in Fig. 1). The TDM represents exchanges of particulate and dis-

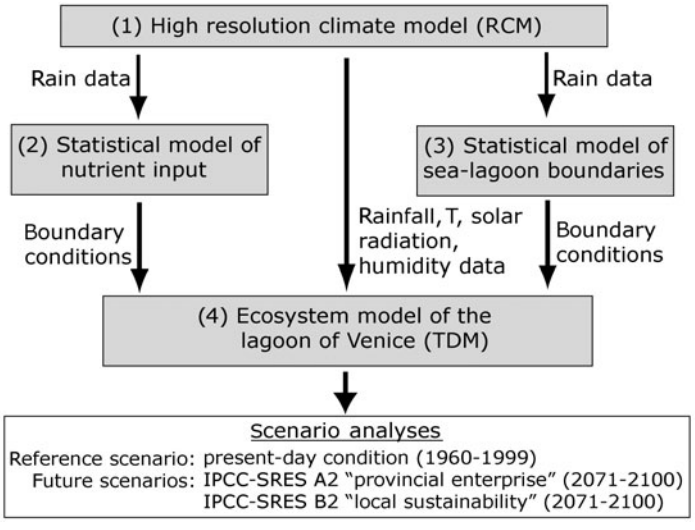

Fig. 2. Downscaling experiment: shaded boxes show models, arrows show the flow of data across models. Models are used for scenario analyses based on the IPCC-SRES emission scenarios (IPCC 2000)

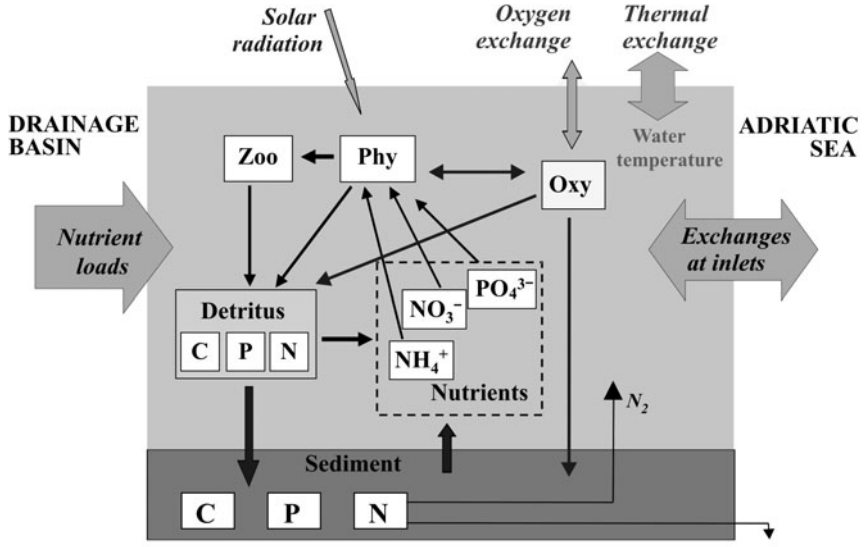

Fig. 3. Transport diffusive model (TDM) of the Venice lagoon: (boxes) state variables, (black arrows) relationships between state variables. Also shown are external forcings (solar radiation, thermal exchange, oxygen exchange) and model boundaries (nutrient loads from the drainage basin, exchanges at the inlets)

solved matter with the Adriatic Sea through the 3 inlets (Fig. 1). It uses a finite difference scheme in which the lagoon is discretized into a regular horizontal grid of 300×300 m and a variable number of vertical layers of 1 m thickness. The integration time step is 1 h, thus daily processes are resolved. A 1 yr simulation takes ~1.5 h of computer time on a Linux AMD opteron64.

TDM has been used for many applications (Pastres et al. 2001, 2005) and process studies (Solidoro et al. 1997, Dejak et al. 1998) and was both calibrated and evaluated against different sets of experimental information (Pastres et al. 2005, Solidoro et al. 2005b). It reproduces timing and magnitude of phytoplankton evolution, spatio-temporal patterns and gradients of nutrient concentrations in agreement with observations (Solidoro et al. 2005b).

2.4. Regional climate model (RCM) and experimental design

The RCM is a 3D primitive equation regional climate model which has been developed over the last 15 yr (Giorgi et al. 1993a, b, Pal et al. 2007) for a wide range of applications (Giorgi & Mearns 1999, Giorgi et al. 2006). The model was run over a domain encompassing the whole Mediterranean basin at 20 km grid spacing (Gao et al. 2006) with lateral boundary conditions provided by corresponding RCM simulations at 50 km grid spacing over the Euro-Mediterranean region (see Giorgi et al. 2004a,b for details). These latter simulations were completed as part of the European project PRUDENCE (Christensen et al. 2002) and were driven at the lateral boundaries by the global climate model HadAM3H (see Giorgi et al. 2004a,b). An assessment of the reliability of the RCM simulation over the drainage basin of the Venice lagoon (Salon et al. 2008) shows that the model has good performance in simulating meteorological variables of relevance to the downscaling procedure, including daily precipitation frequency and intensity statistics.

2.5. Statistical model for nutrient loads

Accurately modeling the nutrient input into the coastal system is a complex task which involves many factors and processes: generation of the load from agriculture and manure, transfer from the soil to groundwater systems and rivers, degradation processes and discharges into the coastal area (de Wit & Bendoricchio 2001, Seitzinger et al. 2002, Uncles et al. 2002, Bouwman et al. 2005). However, considering the aim of the work and the scarcity of observational information on these processes, we chose a simplified approach (detailed in Solidoro et al. 2008a) and summarized as follows.

We begin from the observation that the greater the freshwater runoff, the greater the runoff of nutrients up to a saturation level (de Wit & Bendoricchio 2001, Collavini et al. 2005, Zuliani et al. 2005). Also, we consider the temporal variability of precipitation and the fact that nutrients accumulate in soils and underground waters during dry years, while they are flushed into rivers in wet years (Justić et al. 2005). Therefore, the loads are computed from the rain volume simulated by the RCM using a statistical relationship that makes use of a logarithmic regression between the mean annual precipitation and the estimated total nutrient load, with a saturation effect for high values of annual rainfall.

The statistical regression model between the nutrient loads and rainfall is first constructed from 2001–2003 data, for which estimates of annual loads are available. The model is then applied to the interannual time series of mean annual precipitation over the drainage basin simulated by the RCM in order to obtain a time series of the total annual nitrogen and phosphorus input into the lagoon. The estimated logarithmic relationships for dissolved inorganic nitro-

gen (DIN) and dissolved inorganic phosphorus (PO_4^{3-}) are, respectively:

$$Load_{DIN} = 2845 \cdot \ln(rain) - 15276 \quad (1)$$

$$Load_{PO43-} = 176 \cdot \ln(rain) - 981 \quad (2)$$

The total annual load, calculated for each year of the scenario, is then partitioned among the 10 tributaries according to the proportion of their flows to the total freshwater discharge of the drainage basin (CVN 2005). Then, for each river, the monthly load is computed by subdividing the annual load proportionally to monthly precipitation. The daily value of the load is computed by summing a constant value and a term proportional to the daily precipitation. The constant value is a fixed fraction ($\alpha = 0.60$) of the monthly load normalized by the number of days in each month. The remaining fraction of the monthly load ($1 - \alpha$) is subdivided among the days of the month according to the amount of rain for each day. This empirical formulation is thought to reproduce both the normal flow conditions and the floods induced by heavy rain events.

The generation of nutrients in the drainage basin from non-point sources (e.g. agriculture practices, land cover and manure) is assumed to be fixed and to be equal for the RF and scenario cases. The sensitivity of the results to practices of reduced and increased nutrient generation is also explored (see Section 2.7).

2.6. Statistical model for exchanges at the inlet boundaries

The TDM simulates the exchanges of each state variable at the 3 inlets as a function of mixing coefficients specific to the areas and of the concentration gradient between the inner part of the inlets and the Adriatic Sea. Therefore, time concentration evolutions of TDM state variables at the sea areas close to the inlets are used as boundary conditions of the model.

Evolution of nutrients and phytoplankton concentration at the boundaries is produced based on a combination of climatological evolutions obtained from historical observations and the output of a statistical model that uses the precipitation predicted by RCM. The climatology is constructed by cubic spline interpolation of monthly data from the 6 MELa stations closest to the inlets (see black line in Fig. 4).

The statistical model consists of 4 linear relationships (one for each season) relating mean nutrient concentrations observed in coastal stations and total amount of precipitation (Table 1) for the period 1991–2004. These regressions account for the dependence of seasonal average nutrient concentrations in the northern Adriatic coastal zone on the nutrient loads from the rivers of the Venetian coastline, whose discharges are also related to precipitation patterns. The regression coefficients β_0 and β_1, by variable and season are presented in Table 1 with their p-value. Reliable regressions are found for nitrate, whereas regressions for phosphate and ammonia are less consistent, with $p > 0.40$ in winter and summer for ammonia, and in spring and autumn for phosphate.

The absence of significant relations for phosphate is due to intrinsic weakness of the proposed mechanism and also to the presence of a decreasing trend caused by external factors not related to interannual climate variability. The decreasing trend in concentration PO_4^{3-}

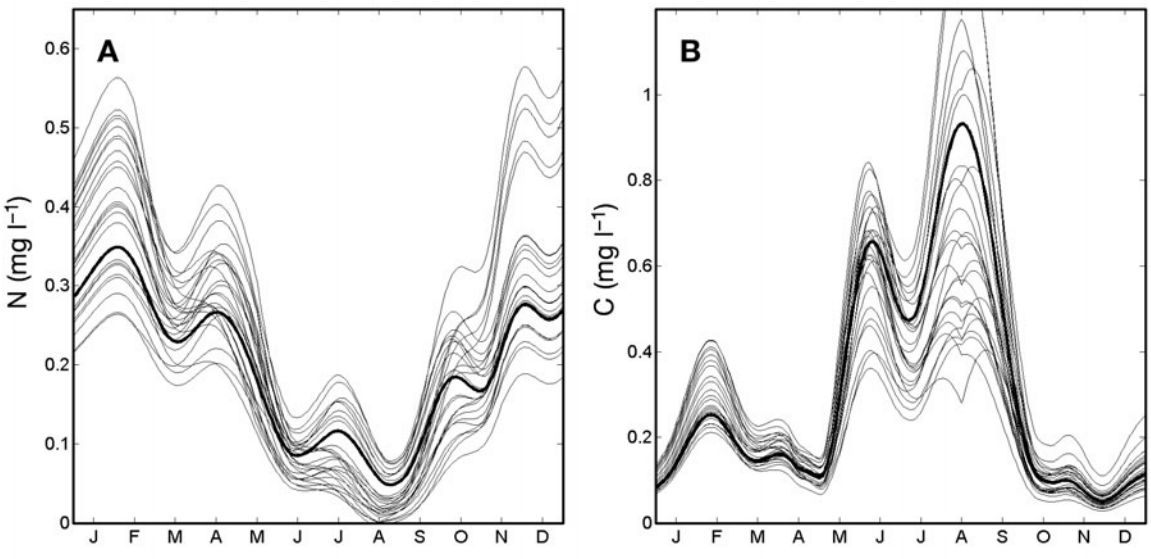

Fig. 4. Climatological evolution of (a) NO_3^-, and (b) phytoplankton at the Venice lagoon–Adriatic Sea boundary (black curves) and boundary conditions for the 30 yr of the reference scenario, obtained as a combination of the climate model output and the result of the statistical regression models (grey curves)

Table 1. Regression coefficients of precipitation effects on mean seasonal nutrient concentrations and phytoplankton, $C = \beta_0 + \beta_1 \times P$, where C is concentration (mg l^{-1}), and P is mean seasonal precipitation (mm)

	Nitrate			Ammonia			Phosphate			Phytoplankton		
	β_0	β_1	p	β_0	β_1	p	β_0	β_1	p	β_0	β_1	p
Winter	0.130	0.00056	0.03	0.0238	−0.00007	0.58	0.0050	0.000016	0.22	0.187	0.00045	0.41
Spring	0.034	0.00056	0.01	0.0064	0.00003	0.43	0.0034	−0.000003	0.54	0.331	0.00011	0.72
Summer	−0.004	0.00028	0.16	0.0076	0.00001	0.79	0.0012	0.00109	0.39	0.008	0.00112	0.05
Fall	0.074	0.00042	0.07	0.0113	0.00002	0.34	0.0060	−0.000009	0.56	0.164	0.00045	0.21

was, in fact, detected in the coastal time series data (Aubry et al. 2004) and can be linked to an estimated decrease in river loads in the last 20 yr (de Wit & Bendoricchio 2001, UNEP/MAP/MED 2003). This in turn is due to reduced use of phosphorus in agriculture and its ban from detergents.

A similar interpretation could be proposed for NH_4^+, for which recent analysis of nutrient data for the Adriatic Sea highlighted the presence of an interannual trend (Solidoro et al. 2008b). However, angular coefficients for the seasonal regressions for ammonia and phosphate are low; thus, changes in rainfall only slightly affect the climatological evolution used at the lagoon–sea boundary. This is the case for all seasons and the 2 nutrients except for phosphate in summer.

Regression for phytoplankton is significant only in summer, whereas phytoplankton is poorly influenced by interannual rainfall variability in other seasons (very low angular coefficients). Therefore, an error noise of normal distribution with zero mean and SD computed from the observations is added to relationships with $p > 0.4$.

Finally, the daily concentration values of the climatological evolution is multiplied by daily weights arising from the ratios between the seasonal concentrations predicted by the statistical regression and the seasonally averaged concentrations of the daily values referring to the same period. As shown in Fig. 4, the daily evolutions of the boundary (grey curves) differ slightly from the climatological pattern for the 30 yr of the present-day simulation.

More details on the parameterization of the boundaries for the scenario simulations are given in Solidoro et al. (2008a).

2.7. Scenario analysis

We consider 5 simulations, as reported in Table 2. The first simulation (BIO-RF) represents the implementation of the present-day conditions. BIO-A2 and BIO-B2 refer to alternative future scenarios of greenhouse gas emissions for the 21st century, A2 and B2, respectively (IPCC 2000). In the A2 scenario, CO_2 concentration grows to ~850 ppm by 2100, while in the B2 scenario projection of CO_2 concentration by the end of the 21st century is ~600 ppm (IPCC 2000).

Two additional scenarios are then considered, BIO-A2+ and BIO-B2– in order to account for possible changes in land use over the drainage basin and implementation of local alternative environmental policies. The 2 scenarios use the same meteorological forcing and boundary conditions as the BIO-A2 and BIO-B2, but different nutrient loads. The BIO-A2+ assumes higher nutrient generation from urban and industrial sources (+50%) and from land/agricultural use (+25%), while the BIO-B2– assumes a decreased nutrient generation from urban and industrial sources (–50%) and from river sources (–25%) as a result of the hypothetical application of new technologies and practices.

These levels of change, although chosen arbitrarily, are reasonable based on the change in nutrient loads

Table 2. Definition of the boundary conditions used in the simulation for the different scenarios. RF, A2 and B2 indicate data from the 3 RCM scenarios that are used as meteorological conditions by the Trophic Diffusive Model (TDM), or are used to estimate exchanges at the boundaries and nutrient inputs from rivers. 2001–2003 mean: historical data used to estimate nutrient inputs from industrial area and urban sources

TDM scenarios	Years	Meteorological condition	Exchanges at inlet boundaries	Nutrient loads	
				River	Urban
BIO-RF	1961–1990	RF	RF	RF	2001–2003 mean
BIO-A2	2071–2100	A2	A2	A2	2001–2003 mean
BIO-B2	2071–2100	B2	B2	B2	2001–2003 mean
BIO-A2+	2071–2100	A2	A2	A2+25%	2001–2003 mean +50%
BIO-B2–	2071–2100	B2	B2	B2–25%	2001–2003 mean –50%

observed in the last 20 yr in the Po river (the largest river in northern Italy), whose drainage basin is similar to that of the Venice lagoon in terms of land use and anthropogenic pressure. In particular, the N load showed an increase from 45×10^6 to 110×10^6 kg yr^{-1} during 1970–1990, while the PO_4^{3-} load showed and increase from ~2.5×10^6 kg yr^{-1} to >5×10^6 kg yr^{-1} during the period 1970–1980 followed by a decrement to 3×10^6 kg yr^{-1} in the 1990s (de Wit & Bendoricchio 2001).

The parameterization of processes and values of the kinetic parameters in the model are the same for all of the simulations: only the climate forcing varies in the different scenarios. The direct effect of temperature changes on the transport processes is considered negligible, while effects on the biological processes are incorporated into the biological model by linking kinetic parameters to recent history of environmental condition. Thus, a first, albeit rough, approximation of biological adaptation to temperature changes is accounted (Solidoro et al. 2008a). With this approach, the effects of temperature variations are minimized, allowing us to better distinguish the effects of changes in precipitation.

3. RESULTS

The TDM is run for 30 yr for the time series of forcing and boundary conditions described in the previous section, i.e. present-day climate conditions (BIO-RF, 1961–1990) and 4 future climate scenarios (BIO-A2, BIO-B2, BIO-A2+ and BIO-B2–, for 2071–2100). Initial conditions for each of the 3 base runs are obtained by running the first year of each simulation 3 times in perpetual mode. The state variable fields of the last simulated day are used as initial conditions.

3.1. Analysis of present-day simulation

This section presents an analysis of the biogeochemical properties of the Venice lagoon ecosystem in the RF simulation, which represents the benchmark for comparison with the future scenario simulations. Model results from the BIO-RF experiment are compared with 3 yr of historical observations from the MELa monitoring project (Solidoro et al. 2005a). This comparison validates the capability of the full downscaling system to reproduce the biogeochemical evolution of the lagoon at this time scale, thereby increasing our confidence on the use of the model to simulate ecosystem biogeochemistry response to future climate scenarios.

Fig. 5 shows the long-term evolution along with the mean annual evolution of DIN, PO_4^{3-} and phytoplankton for the present-day simulations (BIO-RF); moreover, experimental observations are also shown in order to validate the simulated mean annual evolutions. The long-term plots show clear and significant interannual variability in terms of both extreme and mean annual values for all the state variables. The annual mean varies from 0.24 to 0.52 mg l^{-1} for DIN and from 0.008 to 0.02 mg l^{-1} for PO_4^{3-}. Maximum values show a much higher range of variation, from 0.08 to 1.7 mg l^{-1} and from 0.002 to 0.083 mg l^{-1} for DIN and PO_4^{3-}, respectively. The maximum values are observed in winter-autumn and the minimum in summer for DIN and PO_4^{3-}. The average yearly evolutions (right panels) show a clear seasonal pattern for simulated DIN, PO_4^{3-} and phytoplankton, the latter being characterized by a peak in summer, when nutrient concentrations are at the minimum.

Comparison between simulated seasonal evolutions and experimental observations indicates a good agreement for DIN. The DIN spatial variability of the model (grey area in Fig. 5 right panels) is comparable to that of observations except for the winter months and April. The mismatch between simulated and observed variability, particularly in the winter months, is due to high values of few sampling points located close to the river mouths which strongly affect the standard deviation in the observational data set. The model does not reproduce the extreme concentrations observed in the marginal areas of the lagoon during high runoff periods.

The observed average PO_4^{3-} concentration is well reproduced by the model, although the seasonal pattern is not completely matched: simulated November and December values are 20% higher than observations and the observed increase during April and May is not well reproduced. However, the mismatch is within the variability range of the model and the observations.

The typical seasonal cycle of phytoplankton in the Venice lagoon is characterized by a maximum concentration during summer and a minimum in winter. This pattern is well simulated by the model, even though simulated values are 0.5 mg l^{-1} lower than observed in August and 0.3 mg l^{-1} lower than observed in September. The timing of blooms, which generally cover the whole lagoon, is well reproduced. We use the formulation proposed by Cloern et al. (1995) for the conversion of chlorophyll data into carbon units. Since many factors affect the chlorophyll to carbon conversion and the method is sensitive to parameters and light conversion factors, the overall model performance can be considered satisfactory. The model reproduces the mean cycle quite well, while the summer mismatch is within reasonable ranges.

Interannual variability (left panels in Fig. 5) is more evident when looking at the maximum summer levels

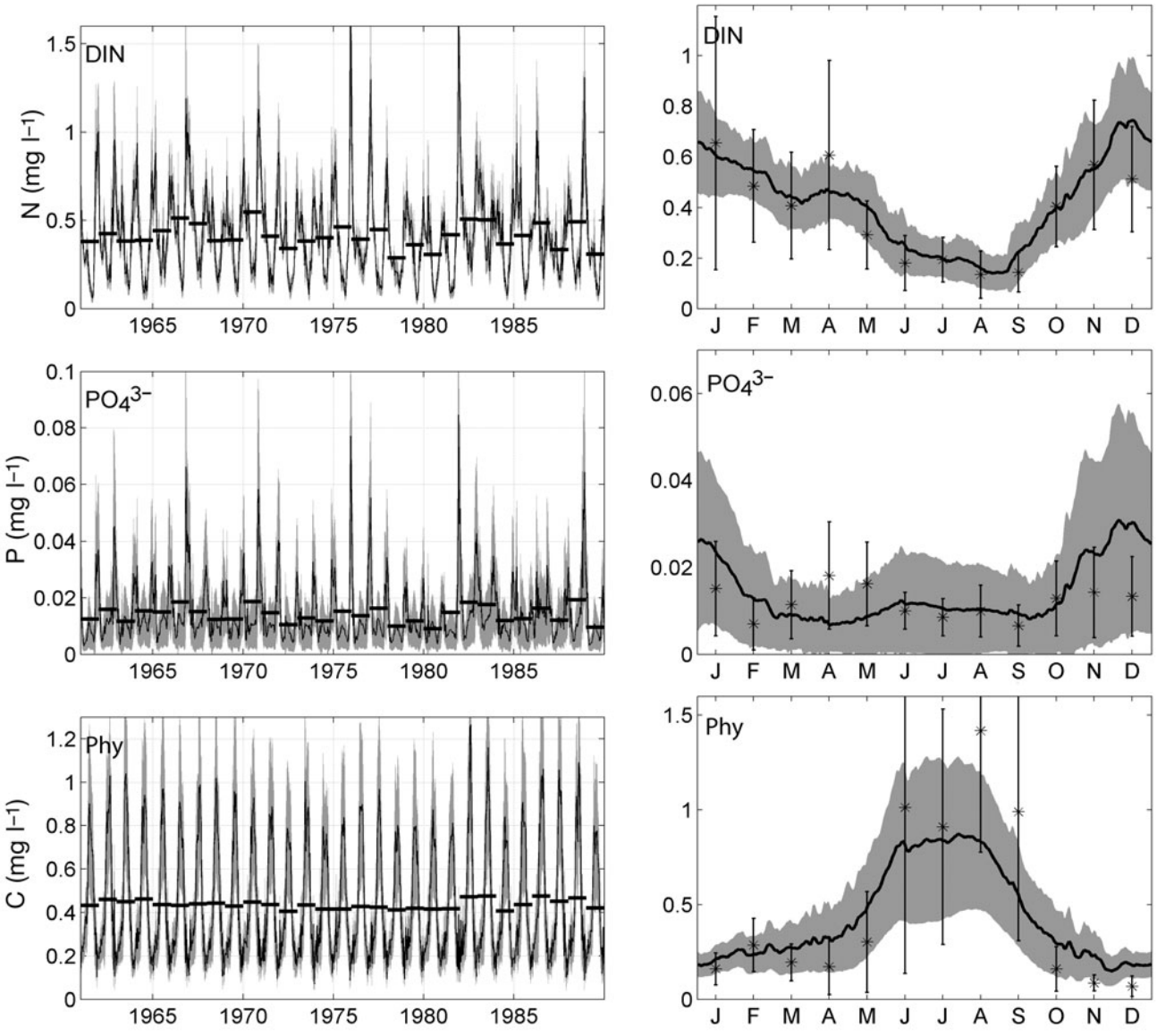

Fig. 5. Left panels: Evolution of DIN (sum of NH_4^+ and NO_3^-), PO_4^{3-} and phytoplankton in the present-day simulation (BIO-RF). The black continuous line is the average computed over the lagoon basin, the gray shaded area shows the SD range of spatial data, and the black horizontal lines show annual means. Right panels: Comparison of model results with historical observations from the MELa monitoring project. The black continuous line is the average of the 30 yr simulation, the gray shaded area shows the simulated spatial SD around the mean evolution, stars and vertical bars are the mean and SD of the monthly MELa data

than the mean annual values because of the skewed distribution of this variable. Indeed, the maximum summer values can vary between 0.78 mg l^{-1} in dry years to 1.22 mg l^{-1} in rainy years. This represents >50% variation around the mean value of the simulation.

The model also reproduces the spatial distribution of DIN and PO_4^{3-} in the lagoon reasonably well. Both the predicted gradients (maps in Fig. 6) and the spatial distribution of observations (filled circles in Fig. 6) are characterized by higher values in the inner parts of the lagoon close to the major discharge points and lower values at the lagoon inlets. Due to the heterogeneous distribution of input from rivers and other point sources along the land–lagoon edge, the northern areas of the lagoon exhibit higher nutrient concentrations than the central and southern areas. The strength of the nutrient gradients is higher in winter and autumn than in summer. The nutrient concentrations over the entire lagoon are generally low and the spatial gradients quite smooth in summer due to the decrease in external input and the enhancement of biological uptake.

The phytoplankton biomass distribution reacts to the availability of nutrients and shows similar patterns. However, since other factors are important (e.g. the

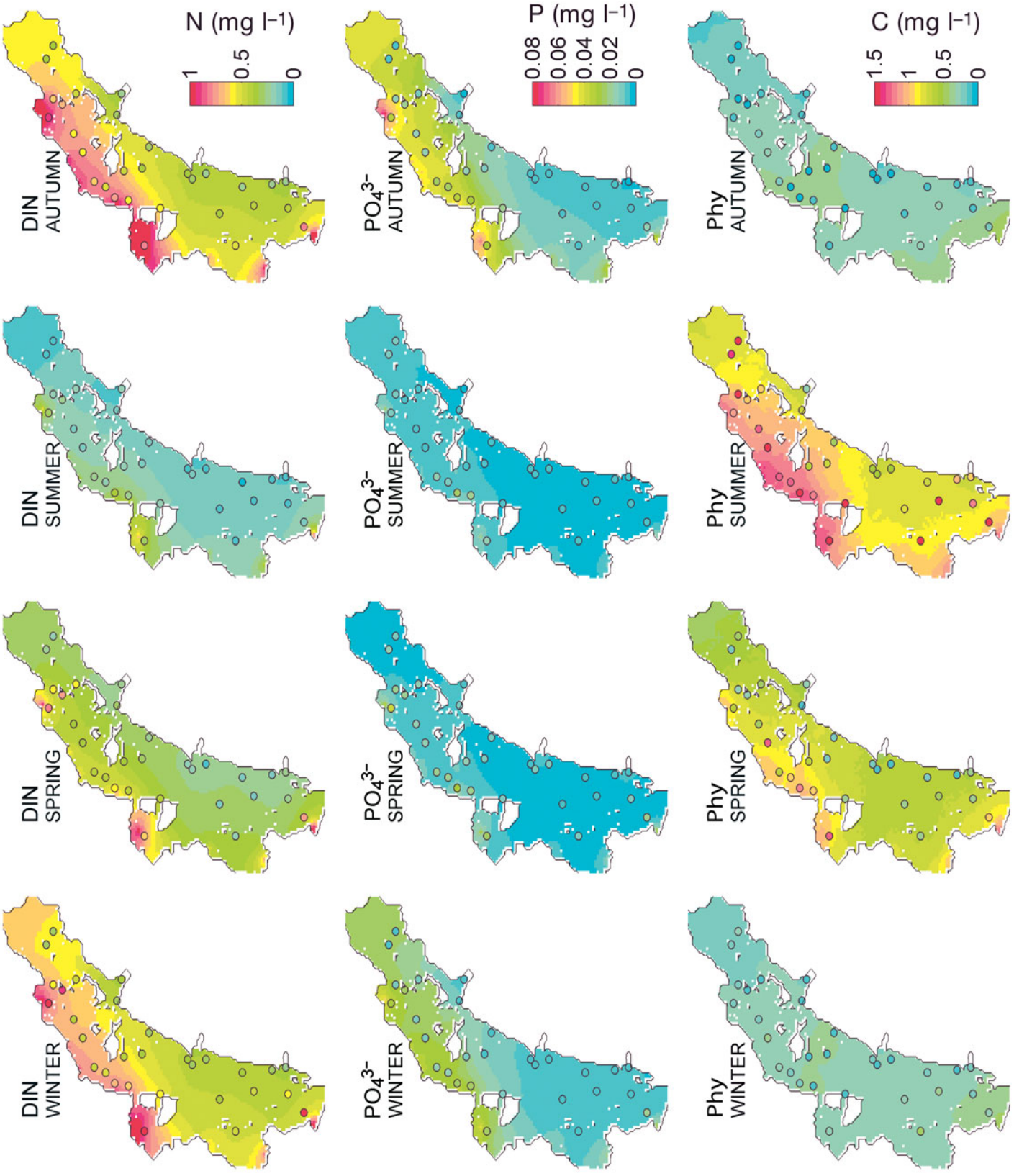

Fig. 6. Seasonal spatial distribution of DIN, PO_4^{3-} and phytoplankton simulated by the BIO-RF scenario (maps). Each map is the seasonal average of the 30 yr for the BIO-RF scenario. Seasonal averages of 2001–2003 MELa observations at the 30 sampling locations are overlaid on the maps (filled circles, same color scale)

residence time in different areas), high concentrations of phytoplankton are also recorded in areas of the lagoon far from the primary nutrient point sources, both in the northern and southern sections of the lagoon (Phy in Fig. 6).

Fig. 7 shows the annual nitrogen budget in the lagoon ecosystem, with annual averages calculated using the 30 yr of the BIO-RF simulation. The phytoplankton primary production is about 33.3 t N d^{-1}, equivalent to ~200 g C m^{-2} yr^{-1}, which makes the lagoon an intermediate to highly productive system (Kennish 2001). Approximately 80% of this flux is recycled to nutrients, either directly or via detritus and sediment compartments. Roughly 28% of the primary production is transferred to secondary producers (zooplankton). In our simplification, this represents the amount of energy available to support higher trophic levels, including fisheries and the mechanical clam harvesting present in the lagoon.

Approximately 40% of the potential available nutrients for primary production is supported by the input from external sources and 60% by the recycling processes, which generates a flux of potential available nitrogen of 26.6 t N d^{-1}. The regeneration of nutrients via microbial activity thus represents a source of nutrients as important as the external input. During the summer season, when the input is low, recycling potentially becomes the most important source of nutrients for the marginal area of the lagoon far from the inlets and input sources. Exchanges with the Adriatic Sea account for 11.3 t N d^{-1}, which is up to 88% of the mean annual input from external sources. The remaining outward fluxes of the nitrogen budget are denitrification and burial processes. These estimates are coherent with those reported in the literature (Solidoro et al. 2005b and references therein).

3.2. Comparison of present-day BIO-RF simulation with future scenarios BIO-A2 and BIO-B2

In this section, we compare results from the future scenario experiments BIO-A2 and BIO-B2 and the reference simulation BIO-RF. Differences emerging from this comparison are only due to the differences in the forcing and boundary conditions that define each scenario, particularly precipitation over the lagoon basin.

As shown by Déqué et al. (2005, 2007), there is general agreement in the simulation of precipitation patterns across the PRUDENCE experiments, although the models employed have a spread in the magnitude and location detail of the patterns. Europe is one of the regions where substantial agreement across models has traditionally been observed.

The projections of future climate simulated by the RCM indicate a slight increase in annual precipitation over the drainage basin of the Venice lagoon relative to the RF. Compared to the RF annual mean of 78 mm mo^{-1}, we find precipitation increases of +3.4 and +6.1 mm mo^{-1} for the A2 and B2 scenarios, respectively. However, the distribution of monthly precipitation variations is not homogeneous, and both future scenarios show a strengthening of the seasonal precipitation cycle, with an increase in autumn and winter/early spring and a decrease in summer (Fig. 8). Moreover, the A2 scenario shows the highest decrement in summer precipitation, while the B2 scenario shows the highest increment in late winter–early spring precipitation.

Precipitation in the A2 scenario is higher than in the RF for the periods January to April and September to November (+30 mm mo^{-1} in October) and lower in June to August (–25 mm mo^{-1} in July). On the other hand, the B2 scenario is characterized by an increase

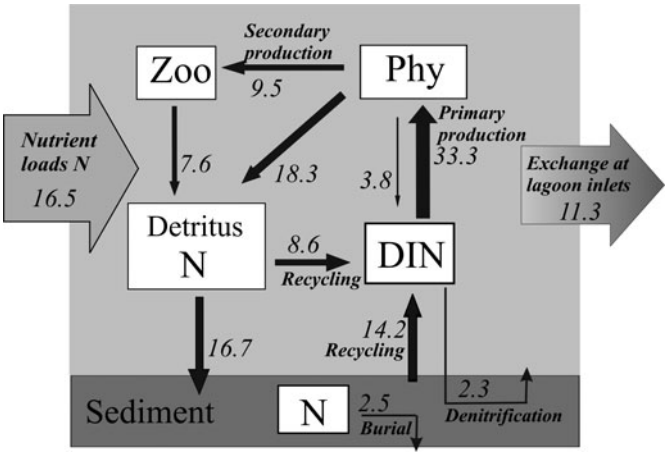

Fig. 7. Annual nitrogen budget for the Venice lagoon obtained from the averages of the 30 yr of the BIO-RF simulation. Fluxes are in 10^3 kg N d^{-1}

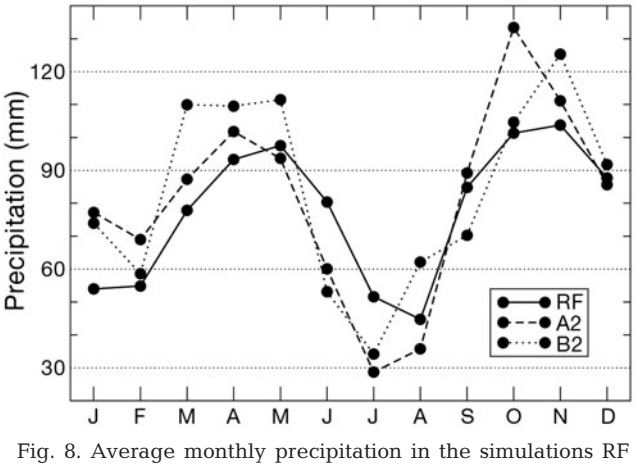

Fig. 8. Average monthly precipitation in the simulations RF (solid line), A2 (dashed line) and B2 (dotted line). Monthly values are obtained by averaging over the 30 yr of each simulation

Table 3. Seasonal means of biogeochemical variables for the BIO-RF simulation (top 4 rows). The other rows show the percentage variation (%) between the future scenarios, BIO-A2 and BIO-B2, and the present-day simulation BIO-RF. Numbers in parentheses are statistical significance (p) of the variations. PP: primary production, PS: secondary production, Winter: JFM, Spring: AMJ, Summer: JAS, and Autumn: OND

		Input N (10^3kg N d^{-1})	DIN (mg N l^{-1})	Phytoplankton (mg C l^{-1})	Zooplankton (mg C l^{-1})	PP (10^3kg N d^{-1})	PS (10^3kg N d^{-1})	Export DIN (10^3kg N d^{-1})
BIO-RF	Winter	14.5	0.558	0.29	0.26	15.0	5.5	−11.0
	Spring	18.1	0.359	0.70	0.46	49.0	14.4	−12.4
	Summer	14.3	0.172	0.92	0.35	52.4	12.6	−9.0
	Autumn	19.0	0.593	0.29	0.27	16.7	5.7	−14.7
BIO-A2	Winter	+12% (0.15)	+12% (0.12)	−2% (0.36)	0% (0.86)	−2% (0.46)	+0% (0.95)	+13% (0.10)
	Spring	−4% (0.49)	−2% (0.81)	−1% (0.34)	+2% (0.66)	0% (0.94)	+1% (0.81)	+1% (0.98)
	Summer	−9% (0.26)	−16% (0.13)	−3% (0.25)	−13% (0.14)	−6% (0.16)	−13% (0.17)	−11% (0.05)
	Autumn	+8% (0.28)	+7% (0.36)	+1% (0.44)	+2% (0.70)	+2% (0.64)	+3% (0.59)	+7% (0.34)
BIO-B2	Winter	+15% (0.04)	+12% (0.03)	0% (0.97)	+3% (0.23)	0% (0.98)	+2% (0.48)	+14% (0.04)
	Spring	−1% (0.92)	+4% (0.63)	0% (0.87)	+6% (0.27)	+3% (0.38)	+5% (0.38)	+7% (0.37)
	Summer	−6% (0.36)	−10% (0.27)	0% (0.84)	−11% (0.20)	−3% (0.49)	−10% (0.24)	−5% (0.19)
	Aut	+6% (0.47)	+3% (0.71)	0% (0.96)	+2% (0.70)	+1% (0.78)	+2% (0.71)	0% (0.96)

in monthly precipitation in January and from March to May. In June to September (except for August), precipitation in the B2 scenario is lower than in the RF (−20 mm mo^{-1} in July).

The impacts of the above variations on the biogeochemical proprieties of the lagoon are summarized in Table 3, which presents the seasonal averages of each state variable and process for the BIO-RF (top 4 rows) and the relative variations for the BIO-A2 (middle 4 rows) and BIO-B2 (bottom 4 rows). The analysis is presented in nitrogen units since this potentially exhibits the largest changes. Indeed, the nutrient loads from river sources account for ~80 and 55% of the respective total loads of DIN and PO_4^{3-} (Solidoro et al. 2005b), and input variations due to precipitation changes only affect riverine sources (urban and industrial loads remain constant).

Changes in the rainfall regime, when processed through the statistical models, imply a seasonal variation in nutrient load, with a decrease in late spring and summer and an increase in winter and autumn for both future scenarios. Due to the seasonal variation in the loads, the mean DIN concentration during spring and summer is lower in both future scenarios than that in the BIO-RF. The decrease is more pronounced in summer than in spring and in the BIO-A2 than in the BIO-B2.

The BIO-A2 scenario shows a decrement in the summer mean DIN concentration of ~0.03 mg l^{-1} (16%) relative to the BIO-RF. This causes a widespread decrease in system productivity and a reduction in phytoplankton and zooplankton biomass. Although the respective declines in phytoplankton biomass and primary production are only 3 and 6%, the impact on secondary production is much higher (−13%). Despite the high interannual variabilities of the evolution of biogeochemical properties simulated within the 2 scenarios, the variations between mean values of BIO-RF and BIO-A2 are significant at $p < 0.30$. In the BIO-B2, the summer decrease in nutrient content does not produce significant changes ($p > 0.30$) in the average phytoplankton biomass and primary productivity (0 and −3%, respectively), but has a significant effect ($p < 0.25$) on zooplankton biomass and secondary production, which decrease by 11 and 10%, respectively. This suggests the dominance of bottom-up control of system productivity during summer. Therefore, the impact of the decrease in nutrient concentration cascades to the highest trophic levels, which suffer the strongest impact.

In spring, despite a slight decrement in nutrient loads, the BIO-B2 scenario shows a small increase in DIN concentration and a relatively larger increase in secondary production as a cascade effect. This is due to the positive changes in nutrient input from January to May, and the accumulation of this nutrient surplus in the lagoon, sustaining a certain increase in production even in June (not shown). In June, the decrease in loads is higher than the sum of the variations of the previous month but its effect becomes visible only at the beginning of summer due to the time lag in model response to input loads.

The simulated increase in nutrient loads results in respective increases in winter and autumn DIN concentrations of 0.07 and 0.04 mg l^{-1} in the BIO-A2 and 0.07 and 0.02 mg l^{-1} in the BIO-B2. However, primary producers do not take advantage of the increased nutrient availability in these seasons since environmental conditions do not sustain plankton productivity. Indeed, mean seasonal values of phytoplankton biomass and primary production in the future scenarios show positive variations <2% which, in absolute terms, are much smaller than those in spring and summer.

The nutrient surplus not utilized by the system results in an increase in nutrient export to the Adriatic Sea. The mean increases in winter DIN fluxes out of

the lagoon are 13 and 14% for the BIO-A2 and BIO-B2 experiments, respectively. In autumn, the increase in outflow is approximately +7% in the BIO-A2, while the increase in nutrient loads does not produce a significant variation in nitrogen export for the BIO-B2.

3.3. Spatial variation of the scenario response

In the future scenario simulations, the response to the changes in input is not spatially homogenous over the lagoon. The obtained DIN variations, both positive and negative, are greater in areas close to discharge point sources. These areas present the highest anomalies, both in terms of absolute values (colour maps of Fig. 9) and relative variations (contour maps of Fig. 9). During winter and autumn, when river outflow is high and biological productivity is low, the positive signal of the variation in river input is diluted by mixing processes, resulting in the absolute and relative variations showing a negative gradient from the rivers towards the inlets. Indeed, the lagoon-sea exchanges play an important role in keeping nutrient concentrations in the lagoon at low levels during these seasons, thus smoothing the impact of increased input in the future scenarios.

In summer, the negative changes over the central areas of the lagoon are less marked (in relative terms) than the ones over the marginal areas close to river mouths, since recycling processes compensate for or attenuate the effects of the decrease in nutrient loads. On the other hand, the relative change remains high (up to –20% in the BIO-A2 and up to –15% in the BIO-B2) over the northernmost portions of the lagoon despite an absolute change as low as approximately –0.05 mg l^{-1}, which is similar to that predicted for the eastern part of the central and southern basins. The northern area is characterized by very low diffusivities and as it is far from any input point, phytoplankton uptake exceeds recycling, and the negative change due to lower input is less efficiently compensated by recycling.

Fig. 10 illustrates the seasonal averages of the changes in secondary production relative to that in the BIO-RF, which can be interpreted as an index of the higher trophic level productivity of the system. The summer and spring patterns are quite similar to those observed for DIN, highlighting the response of system productivity to the change in nutrient availability. Thus, areas that are close to rivers have potentially the largest absolute reduction.

However, a north to south gradient is clearly recognizable in terms of relative values (contour maps). The largest relative changes (up to –15% in summer) are located in the southern part of the basin, while the northern part shows changes of –5 to –10%. The southern part that is characterized by lower productivities, has lower residence times (Solidoro et al. 2004, Cucco & Umgiesser 2006) and higher exchange to volume ratios than the northern part. Thus, exchanges with the Adriatic Sea, which has a lower plankton concentration, enhance the relative impacts of changes in river loads.

The southern part of the basin hosts several important fish farming and clam harvesting activities (Provincia Venezia 2000) which greatly depend on the productivity of the system and could be significantly impacted by the simulated changes in temporal precipitation patterns.

3.4. Analysis of frequency of dry years

Analysis of extreme events is important in understanding climate change effects on the biogeochemistry of the Venice lagoon. Therefore we consider very dry years (see below), particularly the summer season, since it has been shown to be the most active period from a biogeochemical viewpoint. Indeed, phytoplankton productivity can be extremely low during very dry summers. For example, during the extremely dry summer of 2003 (Brunetti et al. 2006), chlorophyll *a* concentrations were 50 to 80% lower than values recorded in previous years (Solidoro et al. 2006).

In the present study we consider the total amount of summer precipitation and use the 25th percentile of the RF distribution, 83 mm $season^{-1}$, as a limit to identify very dry summers. The number of years with precipitation lower than this limit increases by 15% compared to the RF in the A2 scenario, while it decreases by 30% in the B2 scenario, i.e. the A2 scenario is characterized by more frequent dry summers than the B2.

Similarly, it is possible to compute the number of years with mean summer values lower than the 25th percentile of the RF scenario for other state variables and processes (Table 4). Calculations show increased frequencies for the BIO-A2 scenario and significantly decreased frequencies for the BIO-B2. Only zooplankton biomass shows an increase of extreme low years of 15% in both scenarios.

We thus conclude that the BIO-A2 scenario shows a general intensification of extreme events (in terms of dry and low productivity summers) which is not observed in the BIO-B2 scenario. The productivity decrease observed in the BIO-B2 scenario is thus mainly due to a decrease in the other percentiles of the distribution (i.e. in non extreme years).

3.5. Anthropogenic scenarios BIO-A2+ and BIO-B2–

As mentioned, we performed 2 additional scenario simulations in order to test the combined impact of

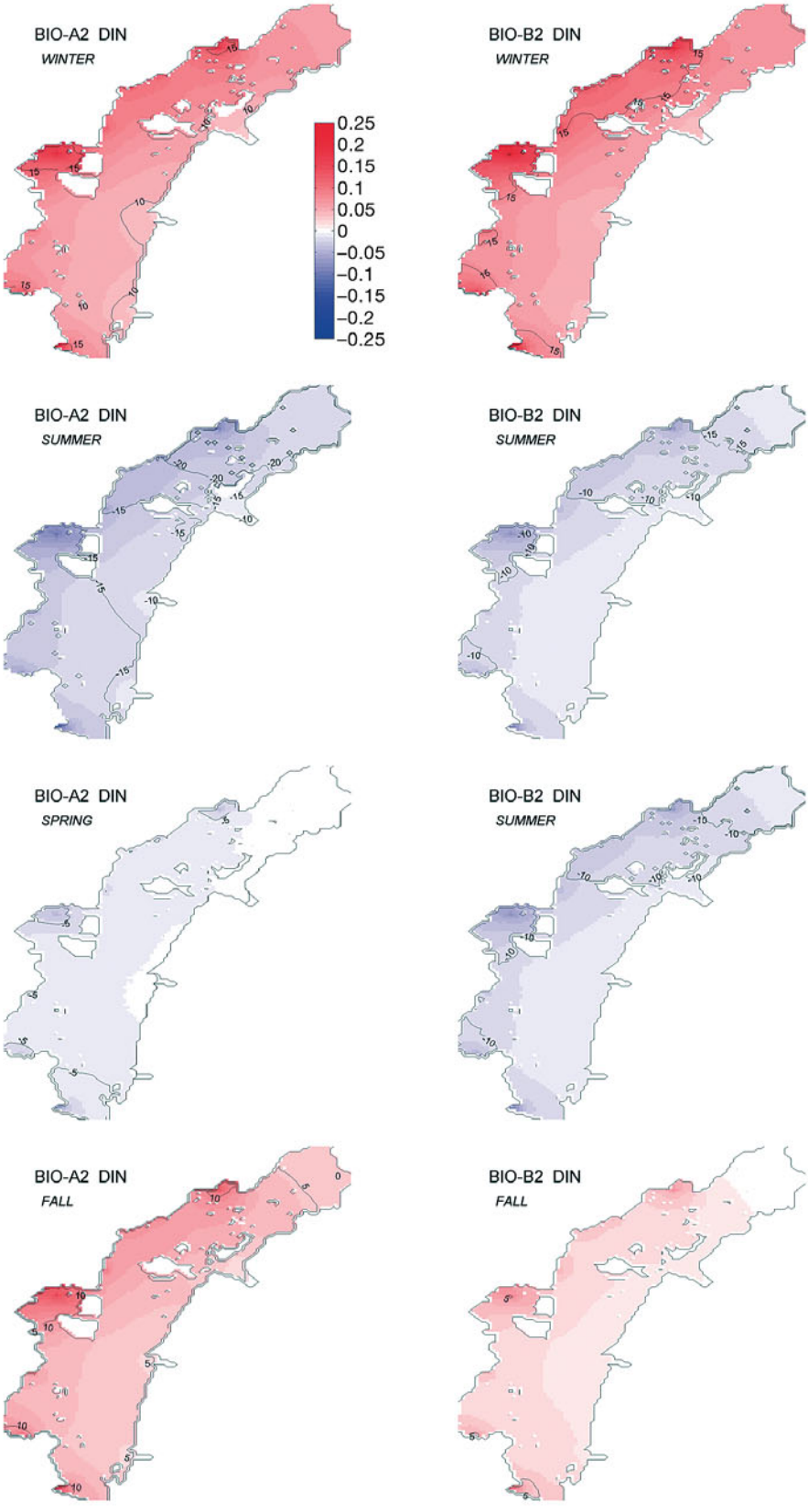

Fig. 9. DIN anomalies of future scenarios with respect to the BIO-RF simulation: (left column) BIO-A2, (right column) BIO-B2. Coloured maps show absolute differences (mg l^{-1}), while overlaid contour maps show relative differences (%)

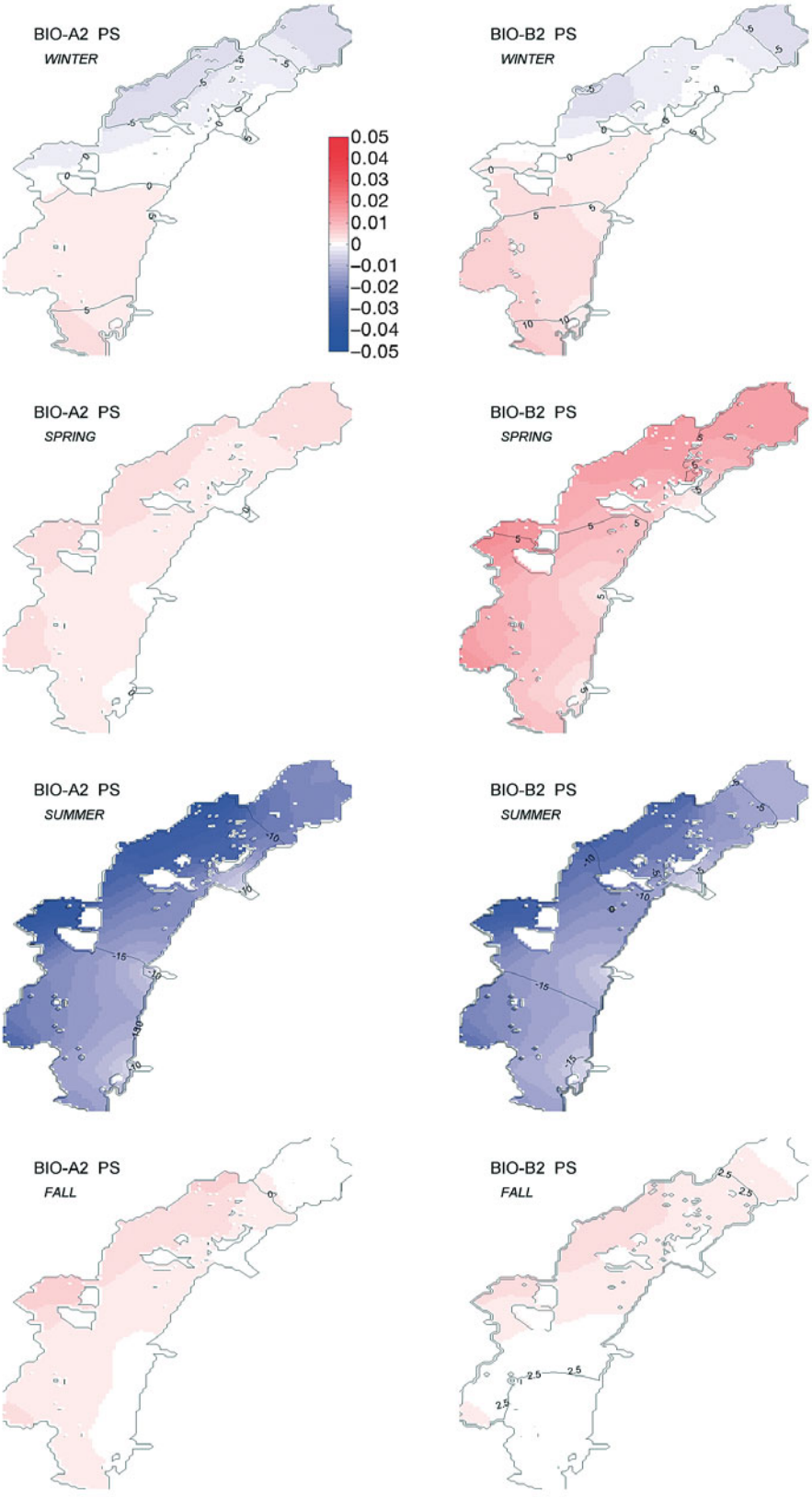

Fig. 10. Secondary production anomalies in the future scenarios with respect to the BIO-RF simulation: (left column) BIO-A2, (right column) BIO-B2. Coloured maps show absolute differences (mg N l^{-1} d^{-1}), while overlaid contour maps show relative differences (%)

Table 4. Number of years for each scenario with summer means lower than that of the 25th percentile, Q25, of the BIO-RF distribution. Q25 values for BIO-RF are given below the column headings. PP and PS: primary and secondary production, respectively

	Rainfall 83 mm	DIN 0.136 mg N l^{-1}	Phytoplankton 0.67 mg C l^{-1}	Zooplankton 0.208 mg C l^{-1}	PP 31.2×10^3 kg N d^{-1}	PS 6.0×10^3 kg N d^{-1}
BIO-RF	7	7	7	7	7	7
BIO-A2	8	8	9	8	7	6
BIO-B2	5	5	3	8	2	5

Table 5. Comparison of seasonal means between the BIO-RF simulation and the future scenarios BIO-A2+ and BIO-B2– (% variation). Numbers in parenthesis are statistical significance (p) of the variations. Absolute values of state variables and fluxes of the BIO-RF are shown in Table 3. PP and PS: primary and secondary production, respectively

		Input N	DIN	Phytoplankton	Zooplankton	PP	PS	Export DIN
BIO-A2+	Winter	46% (0.00)	30% (0.00)	2% (0.46)	8% (0.00)	6% (0.00)	9% (0.00)	51% (0.00)
	Spring	24% (0.00)	14% (0.06)	4% (0.38)	24% (0.00)	14% (0.00)	24% (0.00)	33% (0.00)
	Summer	20% (0.02)	4% (0.74)	2% (0.73)	11% (0.27)	8% (0.11)	12% (0.21)	22% (0.18)
	Autumn	40% (0.00)	29% (0.00)	4% (0.15)	13% (0.00)	11% (0.00)	15% (0.00)	44% (0.00)
BIO-B2–	Winter	–19% (0.00)	–2% (0.68)	–4% (0.01)	–8% (0.00)	–10% (0.00)	–10% (0.00)	–25% (0.00)
	Spring	–30% (0.00)	–12% (0.09)	–6% (0.01)	–18% (0.00)	–13% (0.00)	–19% (0.00)	–27% (0.00)
	Summer	–36% (0.00)	–33% (0.00)	–6% (0.06)	–35% (0.00)	–18% (0.00)	–35% (0.00)	–40% (0.00)
	Autumn	–25% (0.00)	–16% (0.00)	–3% (0.46)	–14% (0.00)	–11% (0.00)	–15% (0.00)	–35% (0.00)

changes in the precipitation regime and changes in land use and management policies (Table 2). Briefly, the simulation BIO-A2+ assumes increased nutrient generation from urban and industrial sources within the A2 climate scenario, while the BIO-B2– assumes a corresponding decrease within the B2 climate scenario. Table 5 shows the seasonal changes for these scenarios relative to the BIO-RF run.

The BIO-A2+ scenario shows a significant increase in all state variables and ecosystem fluxes for all seasons. The positive change in input during spring and summer results in a general increase in the ecosystem productivity. The negative impact previously found in the BIO-A2 scenario is thus more than compensated by the increase in input due to changes in urban sources and by the ecosystem benefits from this additional nutrient availability. Primary production increases by 14 and 8% in spring and summer, respectively, while secondary production increases by 24% in spring and 12% in summer.

The BIO-B2– scenario is characterized by a general decrease (19 to 36%) in loads, and the ecosystem responds to this change by a decrease in all state variables and ecosystem fluxes. The tendency toward oligotrophication of the lagoon during spring and summer induced by climate change effects is strengthened by anthropogenic activities aimed at reducing loads.

The quantification of the reduction or increase in nutrient loads due to anthropogenic practices we tested here, even if based on current literature (de Wit & Bendoricchio 2001), is highly uncertain. However, our sensitivity experiments indicate the direction of the impacts on the lagoon ecosystem and how these compared to the effects of possible climatic changes.

4. CONCLUSIONS

In this paper, we present the development and application of a downscaling system aimed at assessing the potential impact of climate driven changes in precipitation patterns on the biogeochemical properties of the Venice lagoon. The system utilizes a biogeochemical model of the lagoon (TDM), high-resolution meteorological fields from a regional climate model (RCM, Salon et al. 2008), and 2 statistical models that link the meteorological variables to the forcing and boundary conditions of the biogeochemical model.

Three base climate scenarios have been simulated: present-day conditions (RF, 1961–1990), and 2 alternative scenarios for the end of the 21st century (2071–2100) based on the A2 and B2 IPCC-SRES emission scenarios. Both future scenarios show a slight increase in mean annual precipitation over the Venice lagoon drainage basin, although they also exhibit amplification of the seasonal precipitation cycle, with winter and autumn becoming more rainy and summers becoming drier than in the present-day simulation.

The consequences of these precipitation change patterns on the dynamics of the biogeochemical properties of the lagoon were evaluated by running multi-

decadal simulations with the TDM. The decrease in summer precipitation induces a reduction in the nutrient loads, which in turn reduces the productivity of the lagoon system. Such effect is amplified and more easily recognized at the highest trophic levels of the ecosystem. Between the 2 alternative future scenarios, the A2 induces stronger impacts.

On the other hand, the increase in winter and autumn nutrient loads causes an increase in the nutrient concentration in water but has little impact on the eutrophication of the lagoon due to the low productivity of the system during these seasons, which prevent the biological compartments from taking advantage of the enhanced availability of nutrients. Indeed, the nutrient surplus results in an enhancement of the outward fluxes towards the Adriatic Sea.

The northern parts of the lagoon, particularly the zones close to the most important river mouths, show the highest impacts on nutrient concentrations, both in terms of summer reduction and winter-autumn increase. Concerning secondary production, the southern part of the basin, which hosts important aquaculture, fishery and clam harvesting activities, faces the highest percentage changes.

Sensitivity experiments to significant, but still realistic, anthropogenic changes in nutrient loads due to the application of different policies and practices (BIO-A2+ and BIO-B2–) cause impacts on the biogeochemical properties of the lagoon that can overbalance (in positive and negative directions) those induced only by changes in precipitation patterns.

Besides results of interest to the scientific community working on the Venice lagoon, this paper illustrates a hybrid (dynamic and statistical) downscaling methodology for the evaluation of effects of climate changes on biogeochemical properties in a coastal area. The approach might be particularly useful in shallow basins where riverine and continental inputs are among the major forcing functions of the system. Results also demonstrate the feasibility of downscaling experiments even in areas that are very complex to simulate because of the coexistence and interaction of various sources (anthropogenic and natural) of stress and variability.

Acknowledgements. The authors thank M. Bocci and E. Ramieri from Thetis, and L. Montobbio and A. G. Bernstein from Consorzio Venezia Nuova (CVN). The Meteorological Centre of Teolo and Istituto Veneto di Scienze e Arti are acknowledged for providing meteorological data. Regional Agency for Environmental Protection (ARPA) is acknowledged for providing data on trophic variables for the Adriatic Sea and estimates of nutrient loads. CVN is acknowledged for providing the MELa data for the Venice lagoon. This work was partly funded by the Centro Euro-Mediterraneo per i Cambiamenti Climatici (CMCC).

LITERATURE CITED

Bernardi Aubry F, Berton A, Bastianini M, Socal G, Acri F (2004) Phytoplankton succession in a coastal area of the NW Adriatic, over a 10-year sampling period (1990–1999). Cont Shelf Res 24:97–115

Bettiol C, Collavini F, Guerzoni S, Molinaroli E, Rossigni P, Zaggia L, Zonta R (2005) Atmospheric and riverine inputs of metals, nutrients and persistent organic pollutants into the Venice lagoon. Hydrobiologia 550:151–165

Boesch DF, Field JC, Scavia D (2000) The potential consequences of climate variability and change on coastal areas and marine resources. Report of the coastal areas and marine resources Sector Team, U.S. National assessment of the potential consequences of climate variability and change, U.S. Global Change Research Program. NOAA Coastal Ocean Program Decision Analysis Series No. 21, NOAA Coastal Ocean program, Silver Spring, MD

Bouwman AF, Van Drecht G, Knoop JM, Beusen AHW, Meinardi CR (2005) Exploring changes in river nitrogen export to the world's oceans. Global Biogeochem Cycles 19:GB1002

Brunetti M, Maugeri M, Monti F, Nanni T (2006) Temperature and precipitation variability in Italy in the last two centuries from homogenised instrumental time series. Int J Climatol 26:345–381

Christensen JH, Carter TR, Giorgi F (2002) PRUDENCE employs new methods to assess European climate change. EOS Trans Am Geophys Union 83:147

Cloern JE, Grenz C, Vidergar-Lucas L (1995) An empirical model of the phytoplankton chlorophyll:carbon ratio—the conversion factor between productivity and growth rate. Limnol Oceanogr 40:1313–1321

Collavini F, Bettiol C, Zaggia L, Zonta R (2005) Pollutant loads from the drainage basin to the Venice Lagoon (Italy). Environ Int 31:939–947

Cucco A, Umgiesser G (2006) Modeling the Venice Lagoon residence time. Ecol Model 193:34–51

CVN (Consorzio Venezia Nuova) (2005) Technical report of MELa2 project 'Estimation of nutrient and pollutant loads for the estimation for the Venice Lagoon' (in Italian: Aggiornamento al 2003 delle stime dei carichi esterni ed interni e composizione del quadro relativo ai bilanci di massa degli inquinanti in laguna. Progetto: MELa2, linea F. Sviluppo ed aggiornamento dell'analisi dei carichi inquinanti immessi e scambiati in laguna). Consorzio Venezia Nuova, Venezia

Dejak C, Pastres R, Polenghi I, Solidoro C, Pecenik G (1998) 3D modelling of water quality transport processes with time and space varying diffusivity. Coast Estuar Stud 54:645–662

Déqué M, Jones RG, Wild M, Giorgi F and others (2005) Global high resolution versus Limited Area Model climate change projections over Europe: quantifying confidence level from PRUDENCE results. Clim Dyn 25:653–670

Déqué M, Rowell DP, Lüthi D, Giorgi F and others (2007) An intercomparison of regional climate simulations for Europe: assessing uncertainties in model projections. Clim Change 81:53–70

de Wit M, Bendoricchio G (2001) Nutrient fluxes in the Po basin. Sci Total Environ 273:147–161

Gao X, Pal JS, Giorgi F (2006) Projected changes in mean and extreme precipitation over the Mediterranean region from a high resolution double nested RCM simulation. Geophys Res Lett 33:L03706

Giorgi F, Mearns LO (1999) Introduction to the special section: regional climate modelling revisited. J Geophys Res 104:6335–6352

Giorgi F, Marinucci MR, Bates GT (1993a) Development of a second-generation regional climate model (RegCM2). I. Boundary-layer and radiative transfer processes. Mon Weather Rev 121:2794–2813

Giorgi F, Marinucci MR, Bates GT, De Canio G (1993b) Development of a second-generation regional climate model (Reg-CM2). II. Convective processes and assimilation of lateral boundary conditions. Mon Weather Rev 121: 2814–2832

Giorgi F, Bi X, Pal JS (2004a) Mean, interannual variability and trends in a regional climate change experiment over Europe. I. Present-day climate (1961–1990). Clim Dyn 22: 733–756

Giorgi F, Bi X, Pal JS (2004b) Mean, interannual variability and trends in a regional climate change experiment over Europe. II: climate change scenarios (2071–2100). Clim Dyn 23:839–858

Giorgi F, Pal JS, Bi X, Sloan L, Elguindi N, Solmon F (2006) Introduction to the TAC special issue: the RegCNET network. Theor Appl Climatol 86:1–4

Harley CDG, Hughes AR, Hultgren KM, Miner BG and others (2006) The impacts of climate change in coastal marine systems. Ecol Lett 9:228–241

Howarth RW, Swaney DP, Butler TJ, Marino R (2000) Climatic control on eutrophication of the Hudson River estuary. Ecosystems (Intergovernmental Panel on Climate Change) 3:210–215

IPCC (2000) Emissions scenarios. A special report of Working Group III of the Intergovernmental Panel on Climate Change. Cambridge University Press, Cambridge, p 599

Justić D, Rabalais NN, Turner RE (2005) Coupling between climate variability and coastal eutrophication: evidence and outlook for the northern Gulf of Mexico. J Sea Res 54: 25–35

Kennish MJ (2001) Practical handbook of marine science. Institute of Marine and Coastal Sciences, Rutgers University, New Brunswick, NJ

Lehman PW (2004) The influence of climate on mechanistic pathways that affect lower food web production in Northern San Francisco Bay Estuary. Estuaries 27:311–324

Najjar RG (1999) The water balance of the Susquehanna River Basin and its response to climate change. J Hydrol (Amst) 219:7–19

Najjar RG, Walker HA, Anderson PJ, Barron EJ and others (2000) The potential impacts of climate change on the Mid-Atlantic Coastal Region. Clim Res 14:219–233

Neff R, Chang H, Knight CG, Najjar RG, Yarnal B, Walker HA (2000) Impact of climate variation and change on Mid-Atlantic Region hydrology and water resources. Clim Res 14:207–218

Pal JS, Giorgi F, Bi X, Elguindi N and others (2007) Regional climate modelling for the developing world: the ICTP RegCM3 and RegCNET. Bull Am Meteorol Soc 88: 1395–1409

Pastres R, Solidoro C, Cossarini G, Melaku Canu D, Dejak C (2001) Managing the rearing of *Tapes philippinarum* in the Venice lagoon: a decision support system. Ecol Model 138:231–245

Pastres R, Ciavatta S, Cossarini G, Solidoro C (2005) The seasonal distribution of dissolved inorganic nitrogen and phosphorous in the Venice lagoon: a numerical analysis. Environ Int 31:1031–1039

Provincia Venezia (2000) Action plan for the fisheries management in the lagoons of the Venice district (in Italian: Assessorato alla Caccia, Pesca e Polizia Provinciale, Piano per la gestione delle risorse alieutiche delle laguna della provincia di Venezia). Provincia Venezia, Venice

Salon S, Cossarini G, Libralato S, Gao X, Solidoro C, Giorgi F (2008) Downscaling experiment for the Venice lagoon. I. Validation of the present-day precipitation climatology. Clim Res 38:31–41

Scavia D, Field JC, Boesch DF (2003) Forecasting climate impacts on coastal ecosystems. In: Valette-Silver NJ, Scavia D (eds) Ecological forecasting: new tools for coastal and ecosystem management. NOAA Technical Memorandum NOS NCCOS 1:23–28

Seitzinger SP, Kroeze C, Bouwman AF, Caraco N, Dentener F, Styles RV (2002) Global patterns of dissolved inorganic and particulate nitrogen inputs to coastal systems: recent conditions and future projections. Estuaries 25(4b): 640–655

Solidoro C, Brando VE, Dejak C, Franco D, Pastres R, Pecenik G (1997) Long-term simulation of population dynamic of *Ulva r.* in the Venice lagoon. Ecol Model 102: 259–272

Solidoro C, Canu DM, Cucco A, Umgiesser G (2004) A partition of the Venice Lagoon based on physical properties and analysis of the general circulation. J Mar Syst 51: 147–160

Solidoro C, Pastres R, Cossarini G, Ciavatta S (2005a) Seasonal and spatial variability of water quality parameters in the Venice lagoon. J Mar Syst 51:7–18

Solidoro C, Pastres R, Cossarini G (2005b) Nitrogen and plankton dynamics in the Venice lagoon. Ecol Model 184: 103–124

Solidoro C, Pastres R, Cossarini G, Canu DM, Ciavatta S (2006) Order and chaos in the natural world: exploring and understanding variability in the Venice lagoon. Int J Ecodynamics 1:339–347

Solidoro C, Cossarini G, Libralato S, Salon S (2008a) Remarks on the redefinition of system boundaries and model parameterization for downscaling experiments. Prog Oceanogr (in press)

Solidoro C, Bastianini M, Bandelj V, Codermatz R and others (2008b) Current state, scales of variability and decadal trends of biogeochemical properties in the Northern Adriatic Sea. J Geophys Res (in press)

Stenseth NC, Mysterud A, Ottersen G, Hurrell JW, Chan KS, Lima M (2002) Ecological effects of climate fluctuations. Science 297:1292–1296

Struyf E, Van Damme S, Meire P (2004) Possible effects of climate change on estuarine nutrient fluxes: a case study in the higly nutrified Schelde estuary (Belgium, The Netherlands). Estuar Coast Shelf Sci 60:649–661

Suman D, Guerzoni S, Molinaroli E (2005) Integrated coastal management in the Venice lagoon and its watershed. Hydrobiologia 550:251–269

Uncles RJ, Fraser AI, Butterfield D, Johnes P, Harrod TR (2002) The prediction of nutrients into estuaries and their subsequent behavior: application to the Tamar and comparison with the Tweed, UK. Hydrobiologia 475–476: 239–250

UNEP/MAP/MED (2003) POL: riverine transport of water, sediments and pollutants to the Mediterranean Sea. MAP Technical Reports Series No. 141, UNEP/MAP, Athens

Zuliani A, Zaggia L, Collavini F, Zonta R (2005) Freshwater discharge from the drainage basin to the Venice Lagoon (Italy). Environ Int 31:929–938

Editorial responsibility: Mikhail Semenov, Harpenden, UK

Submitted: January 3, 2008; Accepted: July 19, 2008
Proofs received from author(s): November 4, 2008